Available online at www.sciencedirect.com
SCIENCE DIRECT
Polymer 46 (2005) 8306–8312
polymer
www.elsevier.com/locate/polymer

X-ray studies of multiple melting behavior of poly(butylene-2,6-naphthalate)

Munehisa Yasuniwa*, Shinsuke Tsubakihara, Takashi Fujioka, Yusuke Dan

Department of Applied Physics, Faculty of Science, Fukuoka University, Nanakuma 8-19-1, Jonan-ku, Fukuoka 814-0180, Japan

Received 16 February 2005; received in revised form 20 June 2005; accepted 25 June 2005
Available online 19 July 2005

Abstract

Multiple melting behavior of poly(butylene-2,6-naphthalate) (PBN) was studied with X-ray analysis and differential scanning calorimetry (DSC). Double endothermic peaks *L* and *H* attributed to the α-form crystal modification, a small peak attributed to the β-form crystal modification, and a new shoulder peak *S* at a lower temperature of peak *H* appeared in the DSC melting curves. Wide-angle X-ray diffraction patterns of the samples isothermally crystallized at 200 and 220 °C were obtained at a heating rate of 1 K min^{-1}, successively. In this heating process, change of crystal structure and increase of quantity of the β-form crystallites could not be observed up to the final melting. With increasing temperature, the diffraction intensity decreased gradually and then increased distinctly before a steep decrease due to the final melting. The X-ray analysis clearly proved the melt-recrystallization during heating. The β-form crystal modification was formed during slow heating process in the high temperature region.

Keywords: Poly(butylene-2,6-naphthalate); DSC; X-ray

1. Introduction

The double melting behavior of most semicrystalline polymers, such as poly(ethylene terephthalate) [1–3], poly(butylene terephthalate) (PBT) [4–6], poly(butylene-2,6-naphthalate) (PBN) [7–9], poly(phenylene sulfide) [10–12], poly(ether ether ketone) [13–15], and nylon 6 [16], has been investigated extensively. Recently biodegradable polymers, such as poly(L-lactic acid), poly(ethylene succinate), poly(butylene succinate) (PBSu), have been much attention and also shows the double (or multiple) melting behavior [17–21]. The double melting behavior of semicrystalline polymers is usually explained by the melt-recrystallization model [22].

Watanabe reported two crystal modifications of PBN from X-ray analysis [23]. Koyano et al. also carried out the X-ray analysis and precisely determined crystal structures of these modifications [24]. The β-form crystal modification appears under uniaxial sample extension or isothermal (or nonisothermal) crystallization at high-temperature [25,26]. In contrast, the α-form crystal modification appears under normal conditions. Consequently, the melting process of PBN involved the melting attributed to the α- and β-forms. That is, the melting behavior of PBN is complex in comparing with other semicrystalline polymers.

Yasuniwa et al. reported the heating process of an isothermally crystallized PBN sample with X-ray analysis and differential scanning calorimetry (DSC) [9]. DSC melting curves obtained at 10 K min^{-1} showed usual double endothermic peaks and a small endothermic peak due to the melting of the α- and β-forms. Wide-angle X-ray diffraction (WAXD) patterns of a sample isothermally crystallized at 160 °C were obtained, successively. Then, it was concluded from the X-ray analysis that crystal structure of the starting sample (α-form) does not change during heating, and that the increase of the crystallinity, that is recrystallization, occurs before final melting.

As well known, the melting behaviors largely depend on the thermal history of a starting sample [22]. That is, a DSC melting curve considerably changes with isothermal crystallization temperature in the preparation of the starting sample. On the other hand, formation of the β-form has

* Corresponding author. Tel.: +81 92 871 6631; fax: +81 92 865 6030.
E-mail address: yasuniwa@fukuoka-u.ac.jp (M. Yasuniwa).

0032-3861/$ - see front matter © 2005 Elsevier Ltd. All rights reserved.
doi:10.1016/j.polymer.2005.06.072

been reported for samples isothermally crystallized at a high temperature. However, the study of the double melting behavior of PBN in the previous investigation was focused on the sample isothermally crystallized at 160 °C [9]. In this investigation, we studied the melting process of PBN samples isothermally crystallized at various high temperatures, which have high thermal stability, with X-ray analysis and DSC.

2. Experimental

2.1. Sample preparation

Additive free PBN pellets were supplied from Teijin Kasei Co. Ltd (Teijin Kasei PBN TQB-KT77, $[\eta]=0.767$). A PBN sample of about 5 mg was sealed in an aluminum sample pan for DSC. The sample was cooled to an isothermal crystallization temperature (T_c) at a cooling rate of 70 K min^{-1} after holding in the molten state (300 °C) for 10 min, and isothermal crystallization was performed at various T_cs for 1 h. In the case of $T_c=230$ °C, the isothermal crystallization time (t_c) was 2 h, because of a slow crystallization rate at this temperature. Since melting and recrystallization occur competitively in the heating process, melting process depends on a starting temperature of the heating experiment. The samples isothermally crystallized at T_cs were rapidly cooled at a rate of 70 K min^{-1} from T_c to 30 °C. A part of these samples were used for the heating experiment after holding for 10 min at this temperature, and the rest of them were used for the X-ray measurements at an ambient temperature. Hereafter, abbreviated name of ICS (T_c) is used for samples isothermally crystallized at T_c.

2.2. Apparatus

The thermal analysis was carried out with two differential scanning calorimeters, a heat-compensation type (Perkin–Elmer PC-DSC7) and a heat-flux type (TA Instruments TMDSC 2920). The former was used to obtain DSC curves at 10 K min^{-1}, and the latter was used to obtain DSC curves at a slow heating rate (1 K min^{-1}) and the enthalpy change by integration of the DSC curve. The former was also used for the preparation of the ICS. The temperature of these instruments was calibrated with indium and zinc. Samples were always under a nitrogen atmosphere.

WAXD patterns during heating were obtained with an X-ray measurement system reported elsewhere [6]. To obtain refined X-ray diffraction patterns, monochromatized Cu Kα (1.542-Å) radiation was used as an incident X-ray beam with a Rigaku rotating anode X-ray generator. The diffracted X-ray intensity of an isothermally crystallized PBN sample was detected with a position-sensitive proportional counter (PSPC) system. The accumulation time of the PSPC for obtaining one pattern was set to 1 min, and a heating rate was 1 K min^{-1}. That is, the WAXD patterns were obtained at a rate of one pattern per Kelvin. The angles of the diffraction patterns of PBN were corrected with those of α-aluminum oxide (α-Al_2O_3) for the Cu Kα radiation.

3. Results and discussion

3.1. Multiple melting behavior

X-ray analysis was performed for the characterization of the starting sample of DSC. X-ray diffraction patterns of the ICSs (160, 200, and 220 °C) were obtained at room temperature (ca. 20 °C) with our X-ray measurement system and are shown in Fig. 1. The accumulation time of the PSPC of these patterns was 30 min, which was longer than that of the usual measurement (1 min), to obtain refined diffraction patterns.

The crystal structure of the α- and β-forms of PBN has been determined to be triclinic crystal [24]. The Miller index with the α-form crystal structure is given for each diffraction peak in Fig. 1. Arrows shown in the diffraction pattern of $T_c=220$ °C indicate the diffraction peaks assigned to the β-form crystal structure. Obviously, it can be concluded from the diffraction patterns that the ICSs (160 and 200 °C) include only the α-form, and that the ICS (220 °C) includes the α-form and also a small amount of the β-form.

Fig. 2 shows DSC melting curves for the samples isothermally crystallized at T_cs which are indicated in the figure. Heating rate of the DSC scans was 1 K min^{-1}. Because of the slow crystallization rate at $T_c=230$ °C, the ICS (230 °C) was obtained with t_c of 2 h. The authors reported DSC melting curves for ICSs obtained at 10 K min^{-1} in the previous paper [9], and other authors have also reported those for PBN samples obtained at 10 or

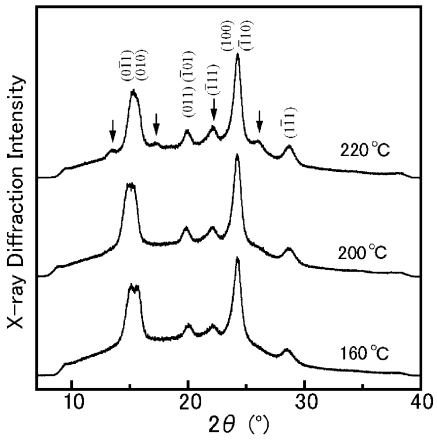

Fig. 1. X-ray diffraction patterns for the ICSs (160, 200, and 220 °C). Arrows indicate the diffraction peaks attributed the β-form crystal modification.

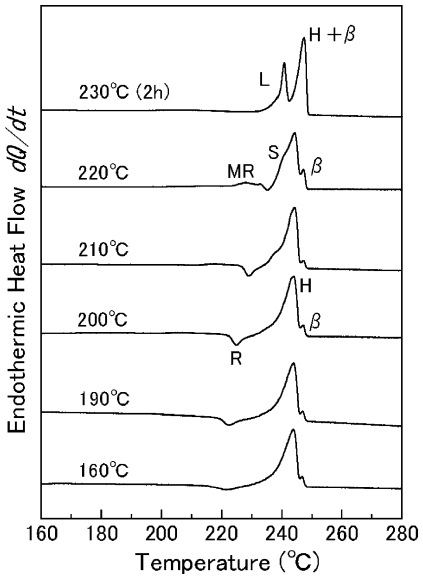

Fig. 2. DSC curves for the ICSs at T_cs which are indicated in the figure. Heating rate of the DSC scans was 1 K min^{-1}.

20 K min^{-1} [8,25,27,28]. The DSC melting curve distinctly changes with the heating rate.

Five endothermic peaks, assigned as *A*, *L*, *S*, *H*, and β appeared in the DSC curve as shown in the figure. Furthermore, an exothermic peak assigned as *R* also appeared in the DSC curve. In this study, $T_m(L)$, $T_m(H)$, $T_m(S)$, and $T_m(\beta)$ stand for the peak melting temperatures of *L*, *H*, *S*, and β, respectively. As mentioned above, the ICSs (160 and 200 °C) include only the α-form, and the ICS (220 °C) includes the α-form and also a small amount of the β-form. Consequently, it is rational to deduce that *A*, *L*, *S*, and *H* correspond to the melting of crystallites having α-form crystal structure.

DSC melting curves shown in Fig. 2 (1 K min^{-1}) and in the previous paper (10 K min^{-1}) indicate that T_c dependence of melting temperatures of *L* and *H*, their T_c dependence of peak areas, and their heating rate dependence agree well with the typical characteristics of the double melting behavior [1–21]. Consequently, *L* and *H* are assigned to the usual double melting peaks. This assignment will be confirmed in the subsequent sections.

Peak *A* also appeared in the DSC curves reported in the previous article [9]. This melting peak has been called 'annealing peak' and is often interpreted as resulting from much poor crystals growing between the larger crystals [22]. Sometimes this peak has been described as 'so-called annealing peak' [29], and models proposed to explain the annealing peak has been given elsewhere [30]. There has been much argument about the origin of the annealing peak, and peak *A* does not have an important role in this article. Therefore, hereafter, this peak is not discussed in this article.

Peak *S* appeared in the DSC curve of $T_c = 220$ °C like a shoulder of peak *H* and decreased with decreasing T_c, whereas *S* disappeared at $T_c = 230$ °C. By the appearance of *S* in the DSC curve for $T_c = 220$ °C, peak *H* decreases, while $T_m(H)$ does not change. These results suggest that two types of crystallites with different thermal stability corresponding to *S* and *H* were formed in the sample. On the other hand, we studied the multiple melting behavior of PBSu and found peak *S* in the DSC melting curves [20,21]. The appearance of *S* has not been reported for other polymers. Further investigation into the origin of *S* was not performed in this study.

Appearance of β-peak in a DSC melting curve of PBN has not been reported in the literatures [8,25,27,28]. A small shoulder peak (β) in the DSC curve was tentatively assigned to the melting of the crystallites having β-form crystal structure in the previous article [9]. This assignment is confirmed in Section 3.3 by X-ray analysis.

β-Form is stable in the high temperature region [25], and a peak temperature of the high temperature endothermic peak for $T_c = 230$ °C in Fig. 2 almost agree with $T_m(\beta)$ in the temperature range lower than 230 °C. Accordingly, it is considered that the high temperature endothermic peak for $T_c = 230$ °C is composed of peaks *H* and β.

3.2. DSC and X-ray analysis of the melting process

Fig. 3(a) and (b) shows X-ray diffraction patterns during heating for the ICSs (200 and 220 °C), respectively. As mentioned in Section 3.1, the ICS (200 °C) includes only the α-form, while the ICS (220 °C) includes the α- and β-forms. As shown in these figures, peak height of the diffraction peaks decreases with temperature, and peak positions shift to lower angle due to the thermal expansion. Except for these changes, a fundamental profile of the diffraction pattern did not change over the whole temperature range, and the increase of the diffraction peak due to the formation of the β-form could not be observed. These facts indicate that α-form crystal structure does not change during heating in the temperature range where X-ray diffraction pattern can be observed.

Assuming that the width of a diffraction peak does not change much in the heating process of the sample, peak height can be used for the diffraction intensity. We used the peak heights for the individual reflection peaks to estimate the quantity of crystallites in the sample, that is, crystallinity, in this article.

Fig. 4 shows temperature dependence of diffraction intensities during heating of (a) ICS (200 °C) and (b) ICS (220 °C). The diffraction intensities for the four dominant peaks, (100), $(0\bar{1}1)$, (010), and $(1\bar{1}1)$ reflections, of the triclinic crystal structure are more intense than the others. As shown in the figure, the diffraction intensities of $(0\bar{1}1)$, (010), and $(1\bar{1}1)$ reflections showed similar temperature dependence among themselves. In a low temperature $(\bar{1}10)$ reflection overlapped on (100) reflection, so that apparent diffraction intensity of (100) reflection was high. Separation of $(\bar{1}10)$ reflection from (100) reflection increased with

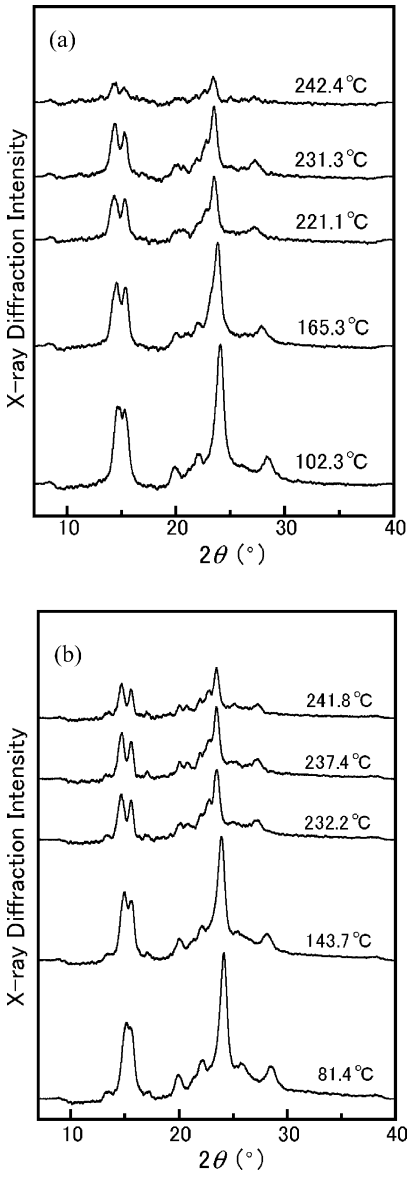

Fig. 3. X-ray diffraction patterns during heating at the rate of 1 K min^{-1} for the (a) ICS (200 °C) and (b) ICS (220 °C).

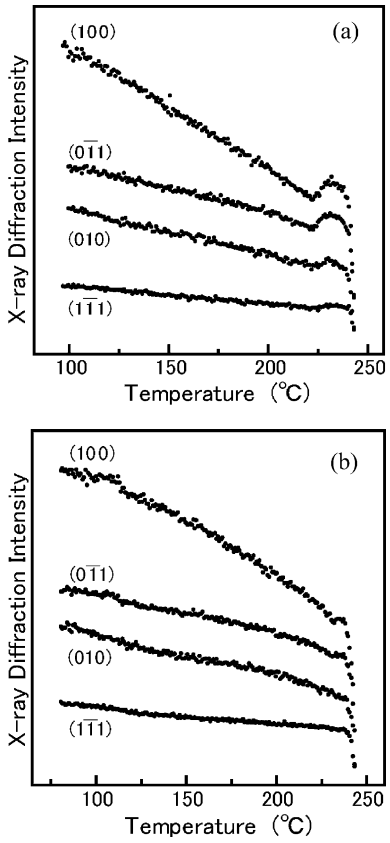

Fig. 4. Temperature dependence of the diffraction intensities for the (a) ICS (200 °C) and (b) ICS (220 °C). The (100), (0$\bar{1}$1), (010), and (1$\bar{1}$1) reflections of monoclinic crystal structure are shown. The heating rate of the DSC scan and the X-ray measurement was 1 K min^{-1}.

increasing temperature, so that the temperature dependence of apparent diffraction intensity of (100) reflection was different from that of the others. The diffraction intensity of (0$\bar{1}$1) reflection is higher than those of (010) and (1$\bar{1}$1) reflections and changes evidently with temperature. Consequently, the (0$\bar{1}$1) reflection is used to estimate the crystallinity of the samples like the previous article [9]. Temperature dependence of the diffraction intensities of (0$\bar{1}$1) reflection, Ix, for the ICSs (200 and 220 °C) are shown in Fig. 5(a) and (b), respectively.

Exothermic heat change $-\Delta Q$ can be obtained from a DSC melting curve by the integration of an exothermic heat flow $-dQ/dt$ and is proportional to the change of crystallinity. Because a change in the X-ray diffraction intensity Ix is approximately proportional to the crystallinity change, temperature derivative curve of the diffraction intensity (dIx/dT) is almost proportional to the heat flow curve, that is $dIx/dT \propto -dQ/dt$. Fig. 5(a) and (b) shows Ix and dIx/dT by dots and dotted line, respectively. For the comparison of the data obtained with WAXD measurements and DSC, the DSC melting curve ($-dQ/dt$) and its integrated curve ($-\Delta Q$) are also shown in the same figure on the same temperature scale by solid line and broken line, respectively. Apparently, Ix and dIx/dT obtained from the X-ray measurements are closely resemble $-\Delta Q$ and $-dQ/dt$ obtained from thermal analysis, respectively.

As shown in Fig. 5(a), X-ray diffraction intensity Ix of the ICS (200 °C) decreased gradually in the low-temperature region and increased abruptly at about 222 °C. Then a positive peak of Ix evidently appeared before final melting. The peak temperature was 232 °C. Because crystallites melt from smaller ones in the heating process on account of their lower thermal stability, it can be considered that the decrease of Ix in the low-temperature region arises from the melting of small crystallites. The appearance of the peak of Ix in the high-temperature region corresponds to an increase in crystallinity in the melting process. Hence, the increase of Ix is interpreted to be a solid proof of the

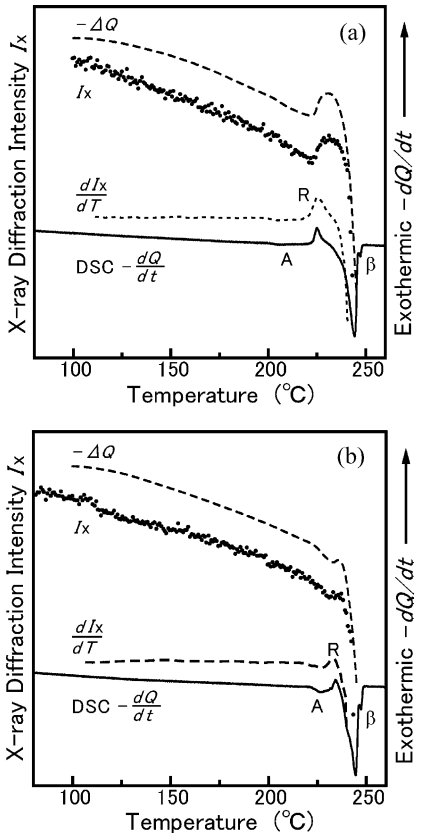

Fig. 5. X-ray diffraction intensity Ix of $(0\bar{1}1)$ reflection, its temperature derivative curve dIx/dT (dotted line), DSC curve $-dQ/dt$ (solid line), and $-\Delta Q$ (broken line) during heating for the (a) ICS (200 °C) and (b) ICS (220 °C). Heating rate of both experiments was 1 K min^{-1}.

recrystallization, and the exothermic peak in the DSC curve can be conclusively attributed to the recrystallization.

As shown in Fig. 5(b), Ix of the ICS (220 °C) also decreased gradually in the low-temperature region and increased at about 231 °C. Then Ix abruptly decreased at about 236 °C. That is, the melting of the sample proceeds immediately after the start of the recrystallization peak. The positive peak of Ix like (a) did not appear. This difference between (a) and (b) can be explained as follows.

Thermal stability of the ICS (220 °C) is higher than that of the ICS (200 °C), that is crystallite size of a starting sample of ICS (220 °C) is larger than that of ICS (200 °C). The melt-recrystallization model [22] suggests that small and imperfect crystals change successively into more stable crystals during heating through the melt-recrystallization mechanism. This means that size distributions of the crystallites of ICS (200 °C) and ICS (220 °C) successively change during heating. However, a rate of the recrystallization decreases with increasing temperature by the molecular motion, therefore, the increase of the crystallite size become rapidly slows down in a high temperature region. As a result, the size distributions of the crystallites of ICS (200 °C) and ICS (220 °C) finally result in a same one, and final melting of ICS (200 °C) and ICS (220 °C) occurs at a same temperature. In the case of ICS (220 °C), melting proceeded immediately after the start of the recrystallization peak, so that the positive peak of Ix like (a) did not appear.

DSC melting curve and X-ray diffraction patterns for the ICS (160 °C) were obtained, and then the correspondences between DSC and X-ray analysis were confirmed in the previous article [9]. The exothermic peak in the DSC melting curve of isothermally crystallized at 200 °C is evidently sharper than that of the ICS (160 °C) as can be seen in Fig. 2. Although the DSC melting curve of the ICS (200 °C) shows a sharp exothermic peak, the curve was well reproduced by a temperature derivative curve of the X-ray diffraction intensity dIx/dT as shown in Fig. 5(a).

3.3. Formation of β-form crystal modification

As shown in Fig. 2, β-peak appeared in all DSC curves whose scanning rate was 1 K min^{-1}, although β-peak in the DSC curves of 10 K min^{-1} disappeared for the ICS ($T_c \leq 225$ °C) as reported in Ref. [25]. These facts indicate that crystallites of the β-form increase during heating with slow heating rate. However, the X-ray diffraction peaks attributed to the β-form did not evidently increase in the temperature range up to 242 °C as shown in Fig. 3. The β-peaks in the DSC curves for the ICSs (200 and 220 °C) appeared at 247.3 °C and were small as shown in Fig. 2. It can be deduced from these results that the β-form grows in the temperature region between 242 and 247.3 °C with slow growth rate.

Chiba et al. studied the crystallization and multiple melting behavior of PBN by the X-ray analysis, Fourier transformation infrared spectroscopy, and DSC [25]. X-ray diffraction peaks attributed to the β-form were not observed in their WAXD patterns for the ICS (220 °C), while they appeared for the ICS (230 °C) and increased with time. They concluded that the β-form appears only at a high temperature region above 230 °C, and they suggested that crystallization does not occur in PBN film at 235 °C. Ju et al. investigated the crystal polymorphism and the multiple melting behavior of PBN prepared by various heat treatments by DSC and WAXD measurements [31]. They obtained WAXD profiles of the ICSs ($t_c = 3$ h) at various temperatures from the melt and showed that the β-form appears for the ICSs ($T_c > 205$ °C). Their result is consistent with our experimental results as shown in Fig. 1.

Fig. 6 shows t_c dependence of X-ray diffraction patterns of the ICSs (220 °C). The diffraction peak heights attributed to the β-form increased with t_c, however, the increase is small. That is, the growth rate of the β-form is considerably slow at 220 °C. Ju et al. also reported t_c dependence of the X-ray diffraction patterns for $T_c = 220$ °C [31]. Their result almost coincides with ours, except that the increase of their peak height with t_c is slightly smaller than that of the present experiment. Since the peak height of the β-form represents the quantity of the β-form crystals, a small difference in the

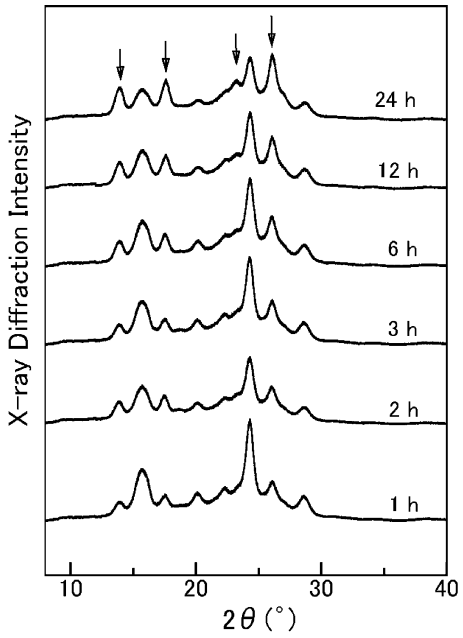

Fig. 6. The t_c dependence of X-ray diffraction patterns for the ICS (220 °C). Arrows indicate the diffraction peaks attributed the β-form crystal modification.

X-ray diffraction intensity between the present result and their one indicates a small difference in the crystal growth of the β-form between them. The growth of polymer crystal mainly depends on experimental conditions (e.g. T_c and t_c) and characteristics of a sample (e.g. molecular weight and structure) [32]. There is no large difference in the experimental conditions between them, so that it is deduced that this small difference in the peak height of the β-form presumably comes from the difference of samples used in the both experiments.

A small endothermic peak due to the melting of β-form crystallites distinctly appears in the DSC melting curves obtained at a heating rate of 1 K min^{-1} as shown in Fig. 2. This endothermic peak results in a shoulder peak of the high temperature peak in the DSC melting curves obtained at 10 K min^{-1} as shown in Fig. 1 of the previous article [9]. Contrary to these results, the endothermic peak of the β-form could not be confirmed in the DSC melting curves obtained at a heating rate of 10 and 20 K min^{-1} reported in Refs. [9,25,27,28]. Accordingly, it can be concluded from these facts that the β-form crystals with higher thermal stability grow in the slow heating process at the high temperature region. As shown in Fig. 2 of this article and in Fig. 1 of the previous article, $T_m(\beta)$s of both ICSs (200 and 220 °C) increased from 242.2 to 247.3 °C by the decrease of the heating rate from 10 to 1 K min^{-1}, respectively. That is, $T_m(\beta)$ increased about 5 K, which was almost the same as the value of the increase of $T_m(H)$ by the decrease of the heating rate from 10 to 1 K min^{-1}. Consequently, it can be interpreted that the growth of the β-form crystals is caused by the increase of $T_m(H)$.

4. Conclusions

The isothermally crystallized PBN showed multiple melting peaks; double melting peaks attributed to the α-form and a melting peak attributed to the β-form. In addition, peak *S* appeared in the DSC curve of $T_c = 220$ °C like a shoulder of peak *H*. The X-ray analysis confirmed that the ICS at T_c higher than 220 °C includes a small amount of the β-form. The β-form peak appeared in all DSC melting curves at a heating rate of 1 K min^{-1}. The WAXD patterns of the ICSs (200 and 220 °C) were successively obtained at a heating rate of 1 K min^{-1}. In the heating process, change of the crystal structure and the increase of quantity of the β-form could not be observed in the X-ray analysis. DSC melting curves for the ICSs (200 and 220 °C) were well reproduced by a temperature dependence curves of the X-ray diffraction intensity. The X-ray analysis clearly proved that the recrystallization occurs during heating, and that the double melting behavior of PBN originates from the recrystallization. It was concluded that the β-form was formed during slow heating process in the high temperature region.

Acknowledgements

The authors would like to thank Teijin Kasei Co., Ltd for providing PBN resins.

References

[1] Holdsworth PJ, Turner AJ. Polymer 1971;12:195.
[2] Zhou C, Clough SB. Polym Eng Sci 1988;28:65.
[3] Tan S, Su A, Li W, Zhou E. J Polym Sci Polym Phys Ed 2000;38:53.
[4] Hobbs SY, Pratt CF. Polymer 1975;16:462.
[5] Cheng SZD, Pan R, Wunderlich B. Makromol Chem 1988;189:2443.
[6] Yasuniwa M, Tsubakihara S, Ohoshita K, Tokudome S. J Polym Sci Polym Phys Ed 2001;39:2005.
[7] Yoon KH, Lee SC, Park OO. Polym J 1994;26:816.
[8] Ju MY, Chang FC. Polymer 2001;42:5037.
[9] Yasuniwa M, Tsubakihara S, Fujioka T. Thermochim Acta 2003;396:75.
[10] Cheng SZD, Wu MY, Wunderlich B. Macromolecules 1986;19:1868.
[11] Chung JS, Cebe P. Polymer 1992;33:2325.
[12] Breach CD, Hu X. J Mater Sci Lett 1996;15:1416.
[13] Cheng SZD, Cao ZQ, Wunderlich B. Macromolecules 1987;20:2802.
[14] Verma R, Marand H, Hisao B. Macromolecules 1996;29:7767.
[15] Wei CL, Chen M, Yu FE. Polymer 2003;44:8185.
[16] Todoki M, Kawaguchi T. J Polym Sci Polym Phys Ed 1977;15:1067.
[17] Yasuniwa M, Tsubakihara S, Sugimoto Y, Nakafuku C. J Polym Sci Polym Phys Ed 2004;42:25.
[18] Al-Raheil IA, Qudah AMA. Polym Int 1995;37:249.
[19] Yoo ES, Im SS. J Polym Sci Polym Phys Ed 1999;37:1357.
[20] Yasuniwa M, Satou T. J Polym Sci Polym Phys Ed 2002;40:2411.
[21] Yasuniwa M, Tsubakihara S, Satou T, Iura K. J Polym Sci Polym Phys Ed 2005;43:2039.
[22] Wunderlich B. Macromolecular physics, crystal melting. vol. III. New York: Academic Press; 1980.
[23] Watanabe H. Kobunshi Ronbunshu 1979;33:229.

[24] Koyano H, Yamamoto Y, Saito Y, Yamanobe T, Komoto T. Polymer 1998;39:4385.
[25] Chiba T, Asai S, Xu W, Sumita M. J Polym Sci Polym Phys Ed 1999; 37:561.
[26] Tsubakihara S, Yasuniwa M. Polym Prepr Jpn 1999;48:4181 [in Japanese].
[27] Papageorgiou GZ, Karayannidis GP. Polymer 1999;40:5325.
[28] Papageorgiou GZ, Karayannidis GP. Polymer 2001;42:2637.
[29] Liu TX. Eur Polym J 2003;39:1311.
[30] Bonnet M, Rogausch K-D, Petermann J. Colloid Polym Sci 1999;277: 513.
[31] Ju MY, Huang JY, Chang FC. Polymer 2002;43:2065.
[32] Wunderlich B. Macromolecular physics, crystal nucleation, growth, annealing. vol. II. New York: Academic Press; 1976.